Chemoprevention of Lung Carcinogenesis by Red Ginseng and Ginsenoside Rg3 in A/J mice

Jie Xiong
Cancer Center, Union hospital, Tongji Medical College, Huazhong University of Science and Technology
Hongmei Yuan
Department of Pathology, Wuhan Jinyintan Hospital
Shihong Fei
Cancer Center, Union Hospital, Tongji Medical College, Huazhong University of Science and Technology
Hongge Wu
Cancer Center, Union hospital, Tongji Medical College, Huazhong University of Science and Technology
Jing Cheng
Cancer Center, Union Hospital, Tongji Medical College, Huazhong University of Science and Technology
Shengli Yang
Cancer Center, Union Hospital, Tongji Medical College, Huazhong University of Science and Technology
Yian Wang
Department of Pharmacology and Toxicology and Cancer Center, Medical College of Wisconsin
Ming You
Department of Pharmacology and Toxicology and Cancer Center, Medical College of Wisconsin
Li Liu (liulist2013@163.com)
Cancer Center, Union Hospital, Tongji Medical College, Huazhong University of Science and Technology

Research

Keywords: red ginseng, ginsenoside, Rg3, P-glycoprotein

Posted Date: August 21st, 2020

DOI: https://doi.org/10.21203/rs.3.rs-63033/v1

Abstract

Background: Red ginseng has long been used as a traditional medicine for a variety of maladies. Ginsenosides are the active components of ginseng but are limited by their low oral bioavailability.

Methods: We evaluated several types of red ginseng extracts for their ability to inhibit lung tumor formation and growth induced by the carcinogen benzo(a)pyrene [B(a)P] in A/J mice. The concentrations of various ginsenosides were quantified in these ginseng extracts using the methods of ultra-performance liquid chromatography tandem mass spectrometry analysis to identify the ginsenosides that may contribute to cancer prevention. We next explored whether inhibition of P-glycoprotein by verapamil could increase the oral bioavailability of ginsenoside by using CaCo-2 cell transcellular transport and in situ mouse intestinal perfusion models. The plasma and intestine concentration of ginsenoside and cancer preventive effect of ginsenoside combined with verapamil in A/J mice were also detected by using B(a)P-induced mouse cancer model.

Results: We found that treatment with one type of red ginseng (Korean red ginseng B, KRGB) led to a significant reduction of tumor load compared with other types of red ginseng. KRGB contained the highest concentration of ginsenoside Rg3 among these red ginseng extracts, suggested that Rg3 may play an important role in its preventive efficacy. Our study showed that Rg3 had a relatively poor bioavailability, and co-administration of verapamil decreased the efflux ratio of Rg3 in Caco-2 cells, increased the absorption rate of Rg3 in rat small intestine, increased the plasma and intestine concentration of Rg3 in A/J mice, and enhanced the cancer preventive effect of Rg3 against B(a)P induced lung tumorigenesis.

Conclusions: Ginsenosides Rg3 is one of the key components of read ginseng that may be responsible for its efficacy against lung carcinogenesis in mice. Rg3 appears to be the substrate of P-glycoprotein, and inhibition of P-glycoprotein could enhance its oral bioavailability.

Background

Lung cancer is associated with the highest incidence and cancer-related mortality in China and North America (1, 2), and non-small cell lung cancer (NSCLC) is the most common type of lung cancer. Smoking, particularly of cigarettes, is the major risk factor for NSCLC (3). Cigarette smoke contains over 60 known carcinogens, including radioisotopes from the radon decay sequence, nitrosamine, and Benzo(a)pyrene [B(a)P] (4). B(a)P is a polycyclic aromatic hydrocarbon and the major toxic constituent of tobacco smoke. Several studies including ours have showed that B(a)P forms DNA adducts in the mouse lung, which are involved in the carcinogenesis of lung cancer, and the B(a)P-induced lung cancer in mice is similar to human lung adenocarcinomas in histopathology and tumor progression stages (5–7). Therefore, B(a)P-induced lung cancer offers a relevant model to study the chemopreventive and anti-cancer effects of natural products.

One potential strategy to prevent lung cancer in high-risk populations is to use chemopreventive agents to regress existing intraepithelial neoplastic lesions, prevent the progression of these lesions to cancer, and inhibit the development of new lesions. A variety of chemopreventive agents have shown efficacies in animal studies (8–9). Our previous studies have found that red ginseng is one of the potential lung cancer preventive agents (10). Ginseng has long been used as a traditional medicine in Asia to improve physical condition and prolong life, and many investigators have demonstrated the antitumor effects of red ginseng (11).

Ginsenosides, also known as ginseng saponins, are the active component of ginseng and usually used as marker compounds for quality assessment of ginseng. some ginsenosides, i.e., Rg1, Re, Rc, Rb2, Rb1, Rd, Rb3, Rh1, Rg3, Rh2, F1, RK1, and Rg5, are commonly used in quantitative measurements of crude ginseng extracts (12–13). In this study, we established a B(a)P-induced lung cancer model in A/J mice for evaluation of the efficacy of different types and batches of red ginseng extracts from China and Korea. These extracts were used for ginsenoside component analysis. Herein we demonstrated for the first time the cancer-preventive activity of red ginseng extract in the mouse model and identified the ginsenosides that may contribute to this activity.

Many active ginsenosides have very poor oral bioavailability (14–15), which may greatly impede the potency of ginsenosides and affect their clinical applications. The mechanism of the low oral bioavailability of ginsenosides is unclear, and P-glycoprotein (P-gp) mediated efflux is reported to be one possible reason (16). P-gp, a member of the ATP-binding cassette superfamily, is one of the most prevalent efflux transporters expressed in multidrug resistance cancer cells and in several organs such as the intestine, liver, kidney, and blood-brain barrier (17). P-gp plays an important role in limiting the intestinal absorption of its substrates, and inhibition of P-gp leads to the improvement of bioavailability of several orally administrated anticancer drugs (16, 18). Some substrates of P-gp, e.g., verapamil and cyclosporine A, have been reported as P-gp inhibitors (19). In this study, verapamil was used as the P-gp inhibitor.

Therefore, the aims of this study were: (1) to investigate the cancer preventive effect of different types of red ginseng extracts in the B(a)P-induced lung tumor mouse model, and to identify the ginsenosides that may contribute to cancer prevention; (2) to demonstrate that inhibition of P-gp by verapamil could increase the oral bioavailability of ginsenoside; and (3) to enhance the cancer preventive effect of ginsenoside through P-gp inhibition using verapamil.

Methods

Animals and reagents

Female A/J mice at 6–7 weeks of age with body weight of 20 ± 1 g were obtained from The Jackson Laboratory (Bar Harbor, ME, USA) and allowed to acclimate to laboratory housing for 1 week before initiating the experiments. Male Wistar rats with body weight of 250 ± 20 g were purchased from the

institution of model animal at Wuhan University (Wuhan, China). Caco-2 cells were obtained from China Center for Type Culture Collection (Wuhan, China). B(a)P and tricaprylin were purchased from Sigma-Aldrich (St. Louis, MO, USA). The Chinese red ginseng (CRG) extract was purchased from Hong Kong Baptist University (Hong Kong, China). The different batches of Korean red ginseng extracts, including Korean red ginseng A (KRGA) extract, Korean red ginseng B (KRGB) extract, and Korean red ginseng C (KRGC) extract were purchased from the Korea Cancer Center Hospital (Seoul, South Korea). Purified ginsenosides Rg3r, Rg3s, and verapamil were purchased from Chengdu Must Bio-Technology Co., Ltd (Chengdu, China).

Administration of red ginseng extracts in B(a)P-treated A/J mice and tumor load measurement in the lung

B(a)P-induced A/J mouse cancer model was established as reported previously (5–6). Animal studies were conducted in accordance with approved protocols by the Institutional Animal Care and Use Committee at the University and were in compliance with the Association for Assessment and Accreditation for Laboratory Animal Care policies. Mice were fed ad libitum and maintained in an environment with a 12-hour light/dark cycle, a temperature range of 65.9-74.1^{0}F, and humidity of 30–70%. At 8 weeks of age, the female A/J mice were given a single intraperitoneal injection of 100 mg/kg B(a)P dissolved in 0.2 mL tricaprylin. One week later, the mice were randomly divided into 5 treatment groups, i.e., control (drinking water), 20 mg/kg CRG, 20 mg/kg KRGA, 20 mg/kg KRGB, and 20 mg/kg KRGC (n = 15 per group). The ginseng extracts were diluted in drinking water and administered once daily via oral gavage. The mice were sacrificed by CO_2 asphyxiation after 20 weeks of treatment. The lungs were collected and fixed in the Tellyesniczky's solution overnight, followed by fixation in 70% ethanol. The fixed lungs were evaluated under a dissecting microscope for surface tumor count and individual tumor size measurement. Tumor volume (V) was calculated using the tumor diameter (r) based on the following formula: V (mm^3) = $4/3\pi r^3$. The total tumor volume was the sum of all tumor volumes in a mouse lung. Tumor load was the averaged total tumor volume in each group. The whole blood and intestine samples were collected and kept at -80^{0}C for ultra-performance liquid chromatography tandem mass spectrometry (UPLC-MS/MS) analysis.

Sample Processing and UPLC-MS/MS Analysis

The red ginseng extracts, blood, and intestine samples from the mouse studies were stored at -80 °C until analysis. The tissues were thawed, weighed, and transferred into a 12 × 75 mm heavy wall glass test tube. A 0.8 mL methanol solution containing internal standards (0.5 μM phloridzin) was added to the test tube. The tissue was homogenized into a homogeneous mixture with a Tissue Tearor and transferred into a 1.5 ml micro-centrifuge tube. The samples were washed twice by the same methanol solution. All solutions were then combined in the centrifuge tube and centrifuged at 15,500 rpm for 15 min. The supernatant (1.0 mL) was removed and dried under nitrogen. The residual was reconstituted in 200 μL methanol for UPLC-MS analysis. A standard curve was prepared in blood with the same procedure, and this curve was used for quantification of all compounds in different tissues as recovery was similar among the tissues.

The UPLC conditions for measuring ginsenosides were: Waters Acquity™ with DAD detector; column: Waters BEH C_{18} column (100 × 2.1 mm I.D., 1.7 μm); mobile phase A: water; mobile phase B (MPB): acetonitrile; gradient for ginseng material analysis: 5% MPB at 0-0.5 min, 5–20% MPB at 0.5-4.0 min, 20–30% MPB at 4.0–5.0 min, 30% MPB at 5.0–12.0 min, 30–50% MPB at 12.0–13.0 min, 50% MPB at 13.0-14.5 min, 50–55% MPB at 14.5–15.0 min, 55% MPB at 15.0–18.0 min, 55–85% MPB at 18.0–20.0 min, 85–95% MPB at 20.0–22.0 min, 95 – 0% MPB at 22.0-22.5 min, and 0% MPB at 22.5–23.0 min; gradient for tissue analysis: 5% MPB at 0-0.5 min, 5–20% MPB at 0.5-1.0 min, 20–80% MPB at 1.0-2.3 min, 80–95% MPB at 2.3–3.5 min, 95 – 5% MPB at 3.6–3.6 min, and 5% MPB at 3.6-4.0 min; Flow rate: 0.45 mL/min; column temperature:, 60^{O}C; injection volume: 10 μL.

MS conditions were API 3200 QTrap triple quadrupole mass spectrometer equipped with a Turbo Ionspray™ source; negative scan mode; ionspray voltage: -4.5 kV; ion source temperature: 650^{O}C; nebulizer gas (gas 1): nitrogen, 50 psi; turbo gas (gas 2): nitrogen 50 psi; curtain gas: nitrogen 10. The quantification was performed by using the multiple reactions monitoring method with ion pair transition to monitor each analyte. Unit mass resolution was set in both mass-resolving quadruple Q1 and Q3. The standard curves for all analytes were linear from 2.5 μM to 19.5 nM. The quality control samples of these compounds were prepared in blood as the same procedure at 312.5 nM. The results revealed that the accuracy values of quality control samples were in the acceptable range (< 15%).

Transcellular transport of Rg3 with or without verapamil in Caco-2 cells

The human colon adenocarcinoma cell line Caco-2 has similar morphological and biochemical characteristics as the human small intestinal enterocytes, and the Caco-2 monolayer has been widely used as a transcellular transport model of the intestinal epithelial barrier. The transcellular transport study was performed as described previously (15). The Caco-2 cells were harvested and seeded on the apical side of a Transwell™ 24-well plate at a density of 1.0 × l0^{5} per well. The confluence of Caco-2 cells within each well was determined by the transmonolayer electrical resistance, and cell confluence would have a Millicell-ERS voltohmmeter reading > 1800Ω.cm^{2}. After 3 weeks of cell culture, the Caco-2 cells were washed three times, and both sides of the monolayer were pre-incubated with HBSS at 37^{0}C. 400 ul of 10 uM Rg3 (Rg3r or Rg3s) or the mixture of 10 uM Rg3 (Rg3r or Rg3s) and verapamil (50 or 100 uM) was loaded to one side of the cell monolayer (the apical or basolateral side), and 600 ul blank HBSS solution was loaded to the other side. After 0, 15, 30, 45, 60, 90, and 120 min, 100 ul media was collected from each receiver compartment and was replaced with preheated 100 ul HBSS. The samples were stored at -4 ^{0}C until UPLC-MS/MS analysis. The apparent unidirectional permeability was obtained according to the equation Papp= (dQ/dT) /A × C0), where dQ/dT is the rate of concentration change in the receiver chamber, A is the surface area of the monolayer (0.6 cm^{2}), and C0 is the starting concentration on the donor side. The permeability from the apical to basolateral side (Pa-b) and the basolateral to apical side (Pb-a) were calculated according to the above equation. The efflux ratio was calculated as Pb-a/Pa-b, which represents the degree of efflux transport of study drug.

In situ intestinal perfusion of Rg3 with or without verapamil

The in situ rat intestinal perfusion study was conducted as described in previous publication (16). Male Wistar rats that were fasted for 24 hours with only free access to water were anesthetized by intravenous injection of 3.5% pentobarbital solution. The small intestine segment was selected for inlet (end of duodenum) and outlet (end of ileum) cannulation with silicone tubes. The inlet tube was pumped at a flow rate of 0.1 mL/min with 10 uM Rg3r or Rg3s in HBSS iso-osmotic solution, using a peristaltic pump. Verapamil solution (50 uM or 100 uM) was mixed with 10 uM Rg3 (Rg3r or Rg3s) to test if it would enhance Rg3 absorption by the intestine. Perfusate samples were collected every 30 min (at 60, 90, 120, 150 min after the start of perfusion) and used for UPLC-MS/MS analysis. The percentage of absorption was calculated using the following equation: Absorption % = (1 - Cout/Cin) × 100%, where Cout and Cin are outlet and inlet perfusion concentrations of Rg3, respectively.

Administration of Rg3 with or without verapamil in B(a)P-treated A/J mice and tumor load measurement in the lung

B(a)P-induced A/J mouse cancer model was established as reported previously. At 8 weeks of age, female A/J mice were given a single intraperitoneal injection of 100 mg/kg B(a)P dissolved in 0.2 mL tricaprylin. One week later, the mice were randomly divided into 6 treatment groups, i.e., control (drinking water), 50 mg/kg verapamil, 10 mg/kg Rg3r, 10 mg/kg Rg3s, 10 mg/kg Rg3r + 50 mg/kg verapamil, and 10 mg/kg Rg3s + 50 mg/kg verapamil (n = 15 per group). The doses were administered once daily via oral gavage for 20 weeks, and the mice were sacrificed by CO_2 asphyxiation. The lungs were fixed and measured for tumor load as described above. The whole blood and intestine samples were collected and kept at -80^{0}C for UPLC-MS/MS analysis as described above.

Statistical Analysis

All the data were represented as mean ± standard deviation, and analyzed by using the GraphPad Prism 7.0 software. The level of statistical significance was set at P value of < 0.05. Significant differences among treatment groups were assessed by Student's t test or one-way analysis of variance.

Results

Preventive effect of different types of red ginseng extract against B(a)P-induced lung cancers in A/J mice

B(a)P-induced mice were treated with drinking water (control), CRG, KRGA, KRGB, or KRGC extract once daily for 20 weeks. No significant body weight loss or clinical signs of toxicity were observed in any treatment groups. The mice were sacrificed at the 20th week after treatment of red ginseng by CO_2 asphyxiation. The lungs from each mouse were fixed, and gross lung tumors in A/J mice treated with different types of red ginseng were shown in Fig. 1A. Light photomicrographs of representative toumor were shown in Fig. 1B. The tumor load was determined by the formula described in the methods. As shown in Fig. 1C, mice treated with KRGB had significant decreases in tumor load compared with the

control group (0.82 ± 0.2 vs. 1.5 ± 0.35, P < 0.05), and the average inhibition rate of tumor load was 45%. There were no significant changes on tumor load after treatments with the other types of red ginseng extracts when compared with the control (P > 0.05).

KRGB contained the highest concentration of ginsenoside Rg3 among 4 red ginseng extracts

The concentrations of various types of ginsenosides, i.e., Re, Rc, Rb1, Rb2, Rb3, Rh1, Rd, Rg1, Rg3, Rg5, F1, and Rk1, were quantified in CRG, KRGA, KRGB, and KRGC using the UPLC-MS analysis. As shown in Fig. 2A, the concentration of total ginsenosides were different amang different ginseng extracts, and CRG showed the highest concentration of total ginsenosides (590.27 ± 41.28umol/L, P < 0.001). The concentration of the each ginsenoside in the different types of red ginseng was shown in Fig. 2B. In particular, KRGB had the highest concentrations of Rg3 (Rg3s: 58.33 ± 3.81 μmol/L and Rg3r: 41.56 ± 2.88 μmol/L) among these 4 red ginseng extracts (P < 0.001), which suggests that Rg3 may be the most important potential cancer-preventive agents against B(a)P-induced lung cancer in A/J mice.

Tissue bio-distribution analysis showed poor oral bioavailability of ginsenosides in mice

After 20 weeks' treatment of the 4 red ginseng extracts, the concentrations of various ginsenosides in the blood and intestine were determined using UPLC-MS/MS. The results showed that only Rg5 was detected in the blood at 0.0063 ± 0.0005 μg/ml after the treatment with KRGB. Other ginsenosides were not detected, indicating poor oral bioavailability and low levels of exposure of these ginsenosides.

Verapamil enhanced the transcellular transport of Rg3 in Caco-2 cells

The Caco-2 monolayer transcellular transport study was performed as described in the methods to investigate if the P-gp inhibitor verapamil could enhance the transcellular transport of Rg3. The transcellular transport of Rg3 (Rg3r and Rg3s) across the Caco-2 monolayer in the absence or presence of verapamil was shown in Table 1. Transcellular transport of Rg3 across the Caco-2 monolayer from the basolateral to apical side was significantly higher than the transport from the apical to basolateral side. The mean *P*a-b of Rg3r was 0.38 ± 0.06. When using the verapamil as P-gp inhibitor, the mean *P*a-b of Rg3r were significantly increased after treatment with 50 and 100 umol/L verapamil, respectively (0.73 ± 0.06 and 1.14 ± 0.09, p < 0.01, and 0.001, respectively). Similar findings could be detected in Rg3s group, indicating that the P-gp inhibitor verapamil could enhance the transcellular transport of Rg3r and Rg3s. The mean values of *P*b-a and efflux ratio of Rg3r and Rg3s were significantly decreased after treatment with 50 and 100 umol/L verapamil (Table 1), indicating that verapamil reduced the outflow of Rg3 across the Caco-2 cell monolayer.

Table 1
Transcellular transport of Rg3 across monolayers of Caco-2 cells in the absence or presence of verapamil

Rg3	Verapamil concentration	*P*a-b (10^{-6} cm/s)	*P*b-a (10^{-6} cm/s)	Efflux ratio (*P*b-a/*P*a-b)
Rg3r	0	0.38 ± 0.06	6.11 ± 0.51	18.26 ± 2.8
Rg3r	50uM	0.73 ± 0.06**	4.18 ± 0.32**	5.77 ± 0.49***
Rg3r	100uM	1.14 ± 0.09***	2.94 ± 0.12***	2.68 ± 0.35***
Rg3s	0	0.54 ± 0.13	7.97 ± 1.30	15.69 ± 3.60
Rg3s	50uM	0.83 ± 0.14*	5.18 ± 1.99**	6.40 ± 1.66***
Rg3s	100uM	0.95 ± 0.19**	3.52 ± 0.79***	3.89 ± 1.22***

Data are presented as mean ± SD of five independent experiments. Permeability and efflux ratio were compared to absence of verapamil. *P□0.05, **P□0.01, ***P□0.001.

Verapamil increased the absorption of Rg3 in the small intestine

In situ rat intestinal perfusion study was used to determine if verapamil could increase the absorption of Rg3 in the small intestine. The rat intestinal absorption model was established as described in the methods. The absorption percentages of Rg3r and Rg3s in the intestinal perfusion at different time points were shown in Fig. 3. The absorption percentage of Rg3r were very poor (about 10%) in the small intestine, and the absorption was significantly increased to over 20% and 25% after treatment with 50 and 100uM verapamil, respectively. Similarly, the absorption of Rg3s significantly increased from 10% to over 20%, and nearly 30% after treatment with 50 and 100uM verapamil, indicating that the P-gp inhibitor verapamil increased the absorption of Rg3r and Rg3s in the small intestine.

Verapamil enhanced the cancer preventive effect of Rg3 in the B(a)P-induced lung cancer mouse model

The B(a)P-induced lung cancer mouse model was established as described in the methods. The B(a)P-treated A/J mice were randomly divided into 6 groups, i.e., drinking water (control), verapamil, Rg3r, Rg3s, Rg3r plus verapamil, and Rg3s plus verapamil groups. The animals were dosed once daily for 20 weeks by oral gavage. No significant body weight loss or clinical signs of toxicity were observed in any treatment group. After 20 weeks treatment, the blood and lung for each mouse were collected. Representative lung tumors in A/J mice treated with different groups were shown in Fig. 4A, and the lung tumor load of different group were shown in Fig. 4B. The tumor load of Rg3r (0.75 ± 0.29 mm^3) and Rg3s (0.81 ± 0.30 mm3) were significantly lower than the control group (1.63 ± 0.40 mm^3, both $p < 0.001$), and the lung tumor load in the Rg3 plus verapamil group was significantly lower than the Rg3 group (0.33 ±

0.25 vs. 0.75 ± 0.29mm^3 for Rg3r, p = 0.0016; 0.29 ± 0.21 vs. 0.81 ± 0.30mm^3 for Rg3s, p = 0.0239), indicating that verapamil enhanced the preventive effect of Rg3 against B(a)P-induced lung cancer. There were no significant differences in tumor load between the verapamil and control group, Rg3r and Rg3s group, or Rg3r plus verapamil and Rg3s plus verapamil group. .

Verapamil increased the plasma concentration of Rg3 in A/J mice

After 20 weeks' treatment, the blood and intestine samples of each group were collected at 24 hours after the last dose administration and analyzed for Rg3 (Rg3r and Rg3s) concentrations using UPLC-MS. The plasma and intestine concentrations of Rg3 were shown in Fig. 4C and Fig. 4D. Co-administration of verapamil and Rg3 significantly increased the plasma and intestine concentration of Rg3 when compared with treatment with Rg3 alone. The plasma concentration of Rg3r plus verapamil group was significantly higher than Rg3r group (1.17 ± 0.47 vs. 0.44 ± 0.32 umol/L, p = 0.0005, Fig. 4C), and intestine concentration of Rg3r plus verapamil was significantly higher than Rg3r group (1.35 ± 0.13 vs. 0.53 ± 0.08 ug/g, p = 0.0001, Fig. 4D). Similar findings could be detected in Rg3s group, indicating that verapamil enhanced the oral bioavailability of Rg3 in A/J mice.

Discussion

In this study, we aim to identify novel and effective chemo-preventive agents for lung cancer, particularly in smokers who are known to be at a high risk. We evaluated the efficacy of several types of red ginseng extracts in preventing B(a)P-induced lung tumorigenesis in A/J mice and found that the KRGB extract significantly reduced the tumor load. We subsequently discovered that KRGB contained the highest concentrations of the Rg3 ginsenosides among the 4 types of red ginseng extracts evaluated in this study, suggesting that Rg3 may be the most important potential cancer preventive effect agent of KRGB.

Ginseng is widely used throughout Asia and North America as a medicinal herb to treat a variety of maladies for a long time (20–22). Several studies have demonstrated that red ginseng has anticancer potential against various tumors (23–25), and several clinical reports have documented the cancer-preventive effect of red ginseng. A case-control study in 905 pairs of Korean patients found that the cancer risk in various organs was decreased almost by half (RR = 0.56) in ginseng takers (26). In another clinical trial conducted in chronic atrophic gastritis patients, administration of red ginseng extract powder for 3 years had significant preventive effects against non-organ-specific human cancers (27).

In this present study, we demonstrated that ginsenoside Rg3 may be the most important potential cancer preventive effect agent in red ginseng. Rg3 has a stereocenter at position C20, giving it two epimers; Rg3r and Rg3s. Both Rg3r and Rg3s significantly reduced the tumor load in the lung of B(a)P treated A/J mice. Rg3r or Rg3s has been studied in several cancer models, and the anti-cancer mechanisms included induction of apoptosis (28, 29), growth inhibition (30, 31), cell cycle arrest (32), and anti-angiogenesis (33, 34). Several studies revealed that Rg3 treatment inhibits metastasis (35, 36) and enhances the

susceptibility of chemotherapy and radiotherapy (37–39). Poon et. al. reported that Rg3s reduced B(a)P-induced genotoxicity in human cells (40). Therefore, Rg3 may be useful for human cancer treatment and have cytoprotective effect against exposure to environmental carcinogens.

Despite the promising cancer preventive potential of ginsenosides, their clinical use has been largely limited by their low oral bioavailability. Several studies have estimated the pharmacokinetic parameters of several ginsenosides after oral adminstion to rats, and the results showed that the bioavailability of ginsenosides was generally under 5% (41–45). Our study also found that only Rg5 was detected at a very low concentration in the blood following treatment with red ginseng extracts for 20 weeks, and the other ginsenosides were not detected because of too low concentration. The reason for the poor bioavailability of ginsenosides is not clear yet. One potential mechanism could be efflux of ginsenosides caused by the P-gp efflux system. Our study is the first to demonstrate that inhibition of P-gp by verapamil can substantially increase the oral bioavailability of Rg3r and Rg3s, suggesting that Rg3 may be a substrate of P-gp, and P-gp may mediate the efflux of Rg3r and Rg3s.

Our study demonstrated that the oral bioavailability of Rg3 was significantly increased in the A/J mice by co-administration with verapamil. The improved bioavailability of Rg3 in the presence of P-gp inhibitor may be due to the enhanced intestinal absorption, which may be attributed to the enhanced transcellular transport of Rg3. Our results showed that the P-gp inhibitor verapamil reduced the outflow of Rg3r and Rg3s across the Caco-2 cell monolayer and enhanced the membrane permeability in Caco-2 cells. Yang et. al. reported that another active ginsenoside Rh2 was also a substrate of P-gp, and its bioavailability was increased from less than 1% to over 30% in mice after co-administration with the P-gp inhibitor cyclosporine A (15). Similar results have been reported for ginsenosides Compound K and Rg1 (46, 47). With co-administration of 2 P-gp inhibitors verapamil and cyclosporine A, the efflux ratio of Compound K was substantially decreased from 26.6 to less than 3 in Caco-2 cells, and the intracellular concentration of Compound K was significantly increased by as much as 40-fold (46). Meng et. al. also reported that verapamil increased the concentration of Rg1 in the rat pulmonary epithelial cells, indicating that P-gp was involved in the efflux of Rg1 (47). However, not all ginsenosides were P-gp substrates. Liang et. al. have showed that the efflux ratios of some ginsenosides, e.g., Rh1, F1, Re, and Rg1, were not affected by verapamil (48). This may be due to the different structures of ginsenosides and existence of other transporters involved in the absorption of certain ginsenosides.

Conclusions

our study revealed that red ginseng had potential of cancer preventive property against B(a)P-induced lung cancer in A/J mice, and ginsenoside Rg3 may contribute to this effect. However, the clinical use of Rg3 was limited by its low oral bioavailability. This is the first report to show that Rg3 may be the substrate of P-gp, and inhibition of P-gp by verapamil significantly enhanced the bioavailability of Rg3 in vitro and in vivo. The cancer preventive effect of Rg3 was enhanced by co-administration of the P-gp inhibitor verapamil, which may be helpful for maximizing the cancer preventive and therapeutic potential of Rg3. Further researches are necessary to investigate the molecular and cellular mechanisms of the

preventive effect of Rg3 against lung cancer and to examine the cancer preventive effect of the combination therapy using Rg3 and P-gp inhibitor in human clinical trials.

Abbreviations

NSCLC
non-small cell lung cancer; B(a)P:Benzo(a)pyrene; P-gp:P-glycoprotein; CRG:Chinese red ginseng; KRGA:Korean red ginseng A; KRGB:Korean red ginseng B; KRGC:Korean red ginseng C; UPLC-MS/MS:ultra-performance liquid chromatography tandem mass spectrometry.

Declarations

Acknowledgements

The authors thanks Dr. Fang Xiefan, from Charles River Laboratories, INC. 6995 Longley Lane, Reno, NV 89511, USA, for medical writing assistance.

Authors' contributions

You ming and Liu li conceived and designed the experiments; Xiong jie, Yuan hongmei and Fei shihong performed experiments; Wu hongge and Chen jing provided experimental support; Yang shengli performed data analyses; Wang yian contributed with stduy design and experimental support; Xiong jie wrote the manuscript; Yang shengli revised the manuscript.

Funding

This work was supported by the national science foundation committee of China (No. 81301800), and clinical medicine and scientific research foundation of Wuhan Municipal Health Commission (No. WX12C09).

Availability of data and materials

All data generated or analyzed during this study are included in this published article and its supplementary information files.

Ethics approval and consent to participate

Animal experiment were approved by the ethics committee of Union Hospital, Tongji Medical College, Huazhong University of Science and Technology

Consent for publication

All materials and images are original. No consent needs to declare.

Competing interests

The authors declare that they have no known competing financial interests or personal relationships that could have appeared to influence the work reported in this paper.

References

1. *Chen W*, *Zheng R*, *Baade PD*, et al. *Cancer statistics in China*, *2015*. *CA Cancer J Clin*. *2016*; *66*: *115 – 32*.
2. *Torre LA*, *Siegel RL*, *Jemal A*. *Lung Cancer Statistics*. *Adv Exp Med Biol*. *2016*; *893*: *1–19*.
3. *Biesalski*, *HK*; *de Mesquita B*, *Chesson A* et al. *European Consensus Statement on Lung Cancer*: *risk factors and prevention*. *Lung Cancer Panel*. *CA Cancer J Clin*. *1998*; *48*: *167 – 76*.
4. *Hecht*, *S*. *Tobacco carcinogens*, *their biomarkers and tobacco-induced cancer*. *Nat Rev Cancer*. *2003*; *3*: *733–44*.
5. *Yan Y*, *Wang Y*, *Tan Q*, *Lubet RA*, *You M*. *Efficacy of Deguelin and Silibinin on Benzo(a)pyrene-Induced Lung Tumorigenesis in A/J Mice*. *Neoplasia*. *2005*; *7*: *1053-57*.
6. *Qi Zhang*, *Huijing Fu*, *Jing Pan*, et al. *Effect of dietary Polyphenon E and EGCG on lung tumorigenesis in A/J Mice*. *Pharm Res*. *2010*; *27*: *1066-71*.
7. *Shi Q*, *Fijten RR*, *Spina D*, et al. *Altered gene expression profiles in the lungs of benzo[a]pyrene-exposed mice in the presence of lipopolysaccharide-induced pulmonary inflammation*. *Toxicol Appl Pharmacol*. *2017*; *336*: *8–19*.
8. *Wen Tan*, *Jinjian Lu*, *Mingqing Huang*, et al. *Anti-cancer natural products isolated from chinese medicinal herbs*. *Chin Med*. *2011*; *6*: *27*.
9. *Zhang Z*, *Wang Y*, *Yao R*, et al. *Cancer chemopreventive activity of a mixture of Chinese herbs (antitumor B) in mouse lung tumor models*. *Oncogene*. *2004*; *23*: *3841–50*.
10. *Yan Y*, *Wang Y*, *Tan Q*, et al. *Efficacy of Polyphenon E*, *Red Ginseng*, *and Rapamycin on Benzo(a)pyrene-Induced Lung Tumorigenesis in A/J Mice*. *Neoplasia*. *2006*; *8*: *52–58*.
11. *Wang CZ*, *Anderson S*, *DU W*, *He TC*, *Yuan CS*. *Red ginseng and cancer treatment*. *Chin J Nat Med*. *2016*; *14*: *7–16*.
12. *Li TSC*, *Mazza G*, *Cottrell AC*, *Gao L*. *Ginsenosides in roots and leaves of American ginseng*. *J Agric Food Chem*. *1996*; *44*: *717–20*.
13. *A S Attele*, J A Wu, C S Yuan.. *Ginseng pharmacology*: *multiple constituents and multiple actions*. *Biochem*. *Pharmacol*. *1999*; *58*: *1685–93*.
14. *Lee Jia*, *Yuqing Zhao*. *Current evaluation of the millennium phytomedicine-ginseng (I)*: *etymology*, *pharmacognosy*, *phytochemistry*, *market and regulations*. *Curr Med Chem*. *2009*; *16*: *2475-84*.
15. *Zhen Yang*, *Song Gao*, *Jingrong Wang*, et al. *Enhancement of Oral Bioavailability of 20(S)-Ginsenoside Rh2 through Improved Understanding of Its Absorption and Efflux Mechanisms*. *Drug Metab Dispos*. *2011*; *39*: *1866-72*.

16. *Jin ZH*, *Qiu W*, *Liu H*, *Jiang XH*, *Wang L*. *Enhancement of oral bioavailability and immune response of Ginsenoside Rh2 by co-administration with piperine*. *Chin J Nat Med*. *2018*; *16*: *143 – 49*.
17. *Sharom FJ*. *ABC multidrug transporters*: *structure*, *function and role in chemoresistance*. *Pharmacogenomics*. *2008*; *9*: *105–27*.
18. *Robert A B van Waterschoot*, *Jurjen S Lagas*, Els Wagenaar, et al. *Absence of both cytochrome P450 3A and P-glycoprotein dramatically increases docetaxel oral bioavailability and risk of intestinal toxicity*. *Cancer Res*. *2009*; *69*: *8996–02*.
19. *Yang K*, *Wu J*, *Li X*. *Recent advances in the research of P-glycoprotein inhibitors*. *Biosci Trends*. *2008*; *2*: *137 – 46*.
20. *Park HJ*, *Kim DH*, *Park SJ*, *Kim JM*, *Ryu JH*. *Ginseng in traditional herbal prescriptions*. *J*. *Ginseng Res*. *2012*; *36*: *225 – 41*.
21. *Yuan CS*, *Wang CZ*, *Wicks SM*, et al. *Chemical and pharmacological studies of saponins with a focus on American ginseng*. *J Ginseng Res*. *2010*; *34*: *160 – 67*.
22. *Choi J*, *Kim TH*, *Choi TY*, *Lee MS*. *Ginseng for health care*: *a systematic review of randomized controlled trials in Korean literature*. *PLoS One*. *2013*; *8*: *e59978*.
23. *Sun S*, *Qi LW*, *Du GJ*, et al. *Red notoginseng*: *higher ginsenoside content and stronger anticancer potential than Asian and American ginseng*. *Food Chem*. *2011*; *125*: *1299-05*.
24. *Wang CZ*, *Aung HH*, *Ni M*, et al. *Red American ginseng*: *ginsenoside constituents and antiproliferative activities of heat-processed Panax quinquefolius roots*. *Planta Med*. *2007*; *73*: *669 – 74*.
25. *Wang CZ*, *Zhang B*, *Song WX*, et al. *Steamed American ginseng berry*: *ginsenoside analyses and anticancer activities*. *J Agric Food Chem*. *2006*; *54*: *9936-42*.
26. *Yun TK*, *Choi SY*: *A case-control study of ginseng intake and cancer*. *Int J Epidemiol*. *1990*; *19*: *871–76*.
27. *Yun TK*, *Zheng S*, *Choi SY*, et al. *Non–Organ-Specific Preventive Effect of Long-Term Administration of Korean Red Ginseng Extract on Incidence of Human Cancers*. *J Med Food*. *2010*; *13*: *489–94*.
28. *Kim BM*, *Kim DH*, *Park JH*, *Na HK*, *Surh YJ*. *Ginsenoside Rg3 induces apoptosis of human breast cancer (MDA-MB-231) cells*. *J*. *Cancer Prev*. *2013*; *18*: *177 – 85*.
29. *Luo Y*, *Zhang P*, *Zeng HQ*, *Lou SF*, *Wang DX*. *Ginsenoside Rg3 induces apoptosis in human multiple myeloma cells via the activation of Bcl-2-associated X protein*. *Mol Med Rep*. *2015*; *12*: *3557–62*.
30. *Li Y*, *Yang T*, *Li J*,et al. *Inhibition of multiple myeloma cell proliferation by ginsenoside Rg3 via reduction in the secretion of IGF-1*. *Mol Med Rep*. *2016*; *14*: *2222–30*.
31. *He BC*.; *Gao JL*, *Luo X*, et al. *Ginsenoside Rg3 inhibits colorectal tumor growth through the down-regulation of Wnt/ss-catenin signaling*. *Int J Oncol*. *2011*; *38*: *437–45*.
32. *Zhang F*, *Li M*, *Wu X* et al. *20 (S)-ginsenoside Rg3 promotes senescence and apoptosis in gallbladder cancer cells via the p53 pathway*. *Drug Des Devel Ther*. *2015*; *9*: *3969-87*.
33. *Kim JW*, *Jung SY*, *Kwon YH*, et al. *Ginsenoside Rg3 attenuates tumor angiogenesis via inhibiting bioactivities of endothelial progenitor cells*. *Cancer Biol Ther*. *2012*; *13*: *504–15*.

34. *Chen QJ*, *Zhang MZ*, *Wang LX*. *Gensenoside Rg3 inhibits hypoxia-induced VEGF expression in human cancer cells*. *Cell Physiol Biochem*. *2010*; *26*: *849–58*.
35. *Junmin S*, *Hongxiang L*, *Zhen L*, *Chao Y*, *Chaojie W*. *Ginsenoside Rg3 inhibits colon cancer cell migration by suppressing nuclear factor kappa B activity*. *J Tradit Chin Med*. *2015*; *35*: *440–44*.
36. *Lee SG*, *Kang YJ*, *Nam JO*. *Anti-metastasis effects of ginsenoside Rg3 in B16F10 cells*. *J Microbiol Biotechnol*. *2015*; *25*: *1997–06*.
37. *Liu TG*, *Huang Y*, *Cui DD*, et al. *Inhibitory effect of ginsenoside Rg3 combined with gemcitabine on angiogenesis and growth of lung cancer in mice*. *BMC Cancer*. *2009*; *9*: *250*.
38. *Kim SM*, *Lee SY*, *Yuk DY*, et al. *Inhibition of NF-kappaB by ginsenoside Rg3 enhances the susceptibility of colon cancer cells to docetaxel*. *Arch Pharm Res*. *2009*; *32*: *755 – 65*.
39. *Wang L*, *Li X*, *Song YM*, et al. *Ginsenoside Rg3 sensitizes human non-small cell lung cancer cells to radiation by targeting the nuclear factor-κB pathway*. *Mol Med Rep*. *2015*; *12*: *609–14*.
40. *Poon PY*, *Kwok HH*, *Yue PY*, et al. *Cytoprotective effect of 20(S)-Rg3 on Benzo(α)pyrene-induced DNA damage*. *Drug Metab Dispos*. *2011*; *40*: *120 – 29*.
41. *Li H*, *Ye M*, *Guo H*, et al. *Biotransformation of 20(S)-protopanaxadiol by mucor spinosus*. *Phytochemistry*. *2009*; *70*: *1416-20*.
42. *Paek IP*, *Moon Y*, *Kim J*, et al. *Pharmacokinetics of a ginseng saponin metabolite compound K in rats*. *Biopharm Drug Dispos*. *2006*; *27*: *39–45*.
43. *Xu QF*, *Fang XL*, *Chen DF*. *Pharmacokinetics and bioavailability of ginsenoside Rb1 and Rg1 from Panax notoginseng in rats*. *J Ethnopharmacol*. *2003*; *84*: *187 – 92*.
44. *Gu Y*, *Wang GJ*, *Sun JG*, et al. *Pharmacokinetic characterization of ginsenoside Rh2, an anticancer nutrient from ginseng, in rats and dogs*. *Food Chem Toxicol*. *2009*; *47*: *2257-68*.
45. *Qian T*, *Cai Z*, *Wong RN*, *Mak NK*, *Jiang ZH*. *In vivo rat metabolism and pharmacokinetic studies of ginsenoside Rg3*. *J Chromatogr B Analyt Technol Biomed Life Sci*. *2005*; *816*: *223 – 32*.
46. *Zhen Yang*, *Jing-Rong Wang*, *Tao Niu*, et al. *Inhibition of P-glycoprotein leads to improved oral bioavailability of Compound K, an anti-cancer metabolite of red ginseng extract produced by gut microflora*. *Drug Metab Dispos*. *2012*; *40*: *1538-44*.
47. *Zhen Meng*, *Hongyin Zhang*, *Yunan Zhao*, *Jiaqi Lan*, Lijun Du. *Transport behavior and efflux of Rg1 in rat pulmonary epithelial cells*. *Biomed Chromatogr*. *2007*; *21*: *635–41*.
48. *Yan Liang*, *Yuanyuan Zhou*, *Jingwei Zhang*,et al. *Pharmacokinetic Compatibility of Ginsenosides and Schisandra Lignans in Shengmai-san*: *From the Perspective of P-Glycoprotein*. *PLoS One*. *2014*; *9*: *e98717*.

Figures

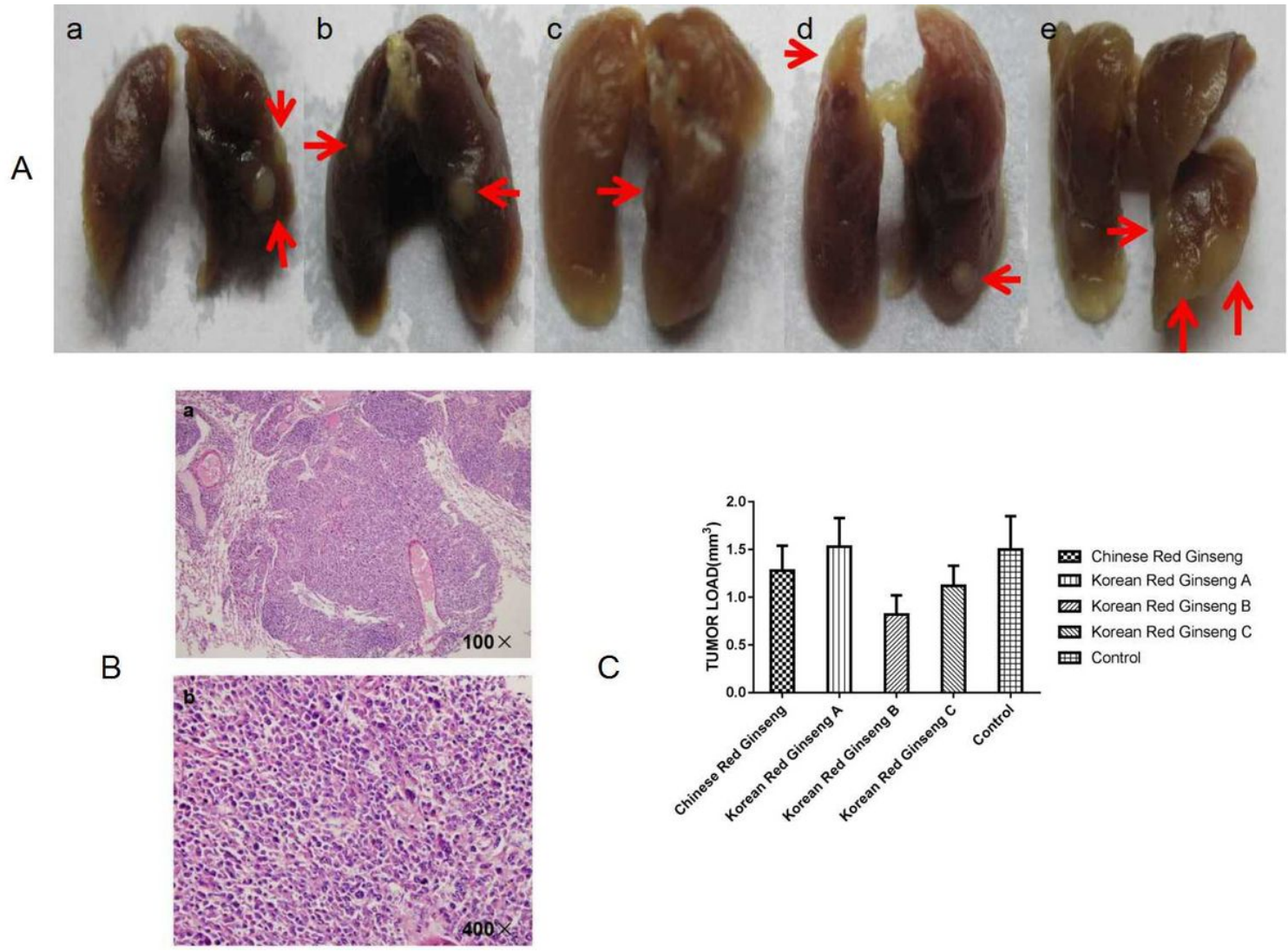

Figure 1

Chemopreventive effect of lung carcinogenesis by different types of red ginseng in A/J mice. (A) Gross lung tumors in A/J mice treated with different types of red ginseng. Arrows indicate tumors. a: Chinese red ginseng group. b: Korean red ginseng A group. c: Korean red ginseng B group. d: Korean red ginseng C group. e: Control group. (B) Light photomicrographs of representative toumor in lung. a: at 100 magnification. b: at 400 magnification. (C) Effects of different types of red ginseng on tumor load. Error bars represent the mean ± SD.

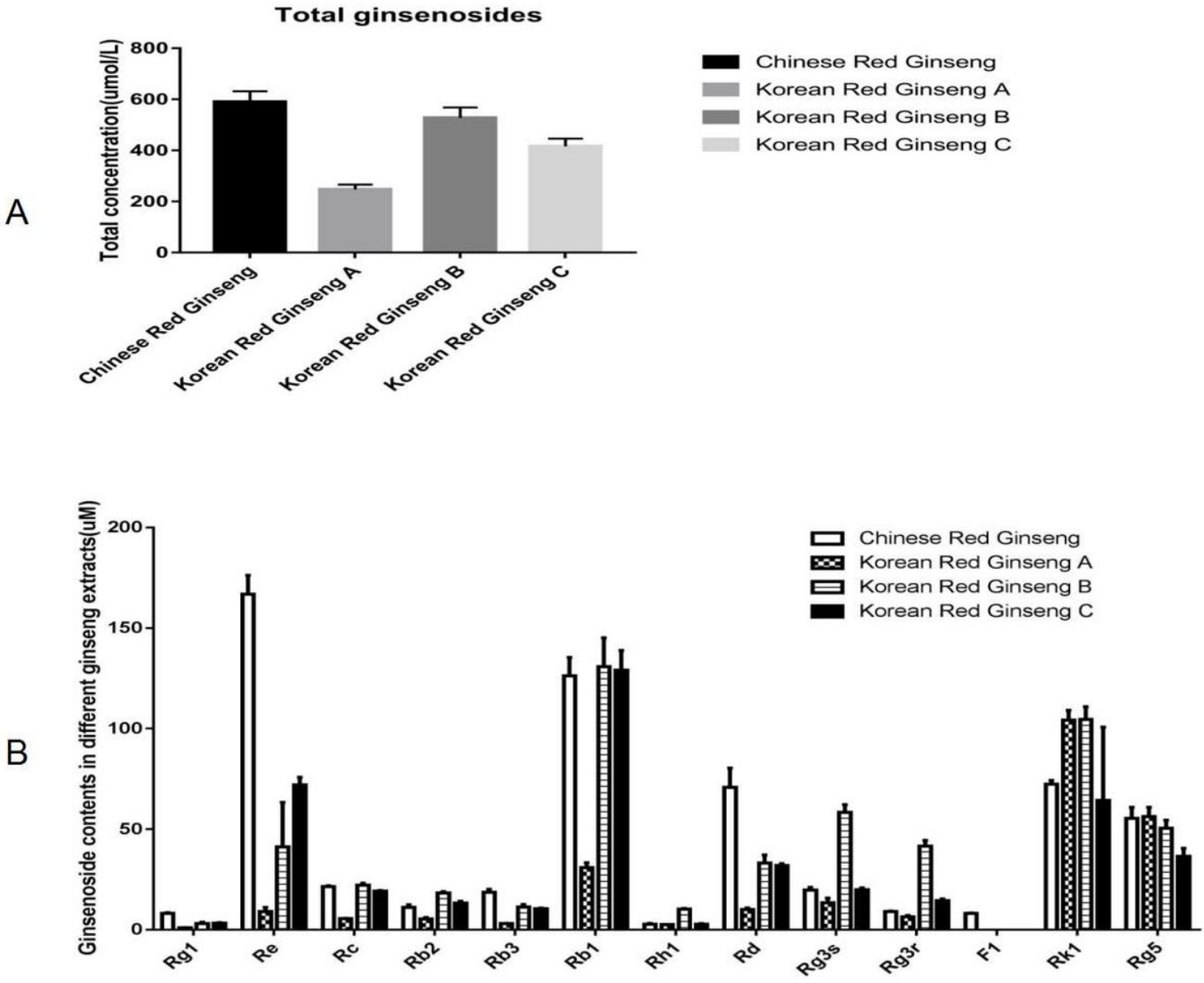

Figure 2

Ginsenoside concentrations detected in different red ginseng extracts. (A)Total ginsenosides detected in the drinking water of different red ginseng extracts (10 mg/ml). 13 ginsenosides were measured. Error bars represent the mean ± SD of three independent experiments. (B) Each ginsenoside detected in the drinking water of different ginseng extracts. Error bars represent the mean ± SD of three independent experiments.

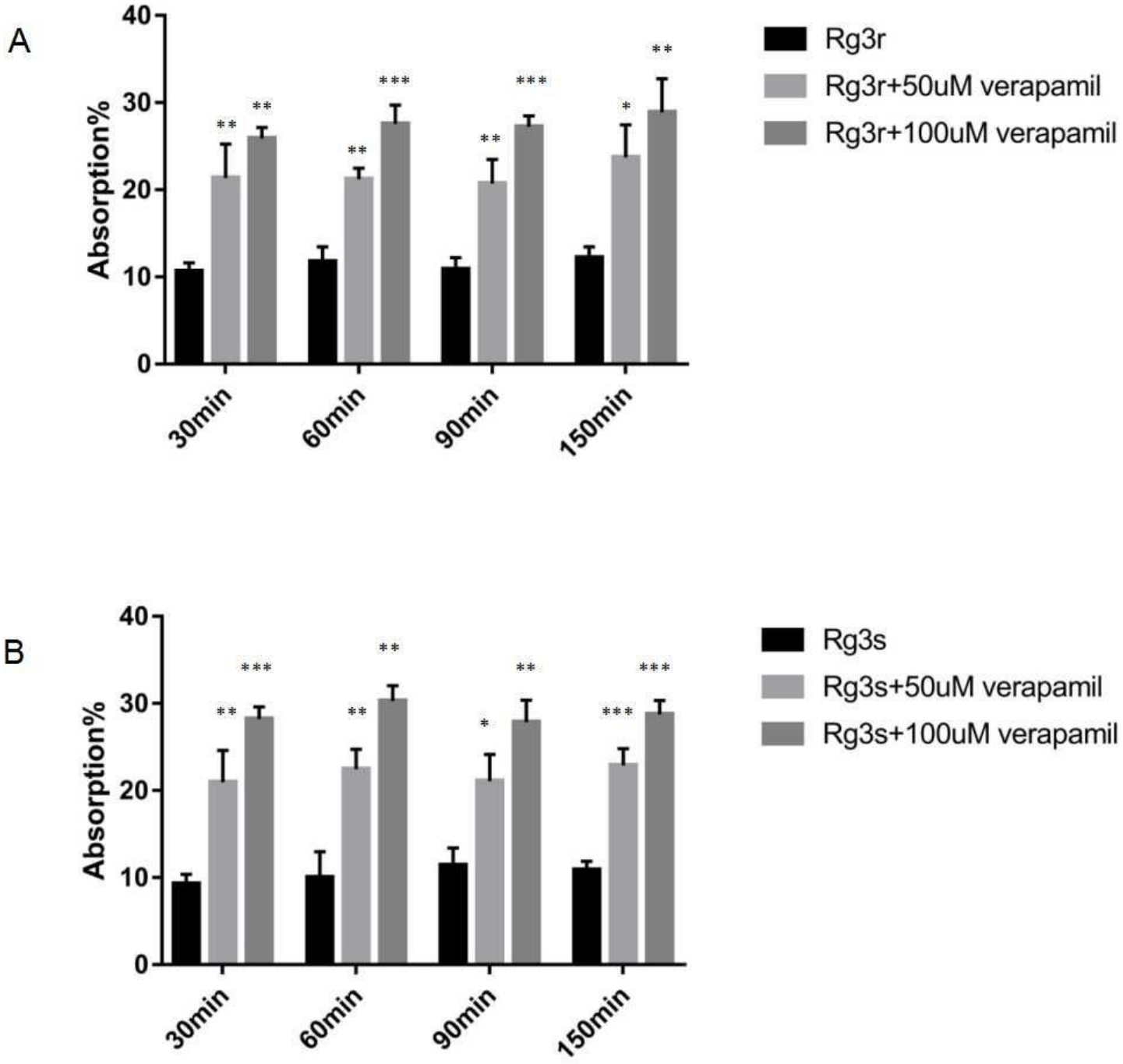

Figure 3

Absorption percentages of Rg3 in intestinal perfusion in wistar rats. (A) Rg3r groups, (B) Rg3s groups. Data are presented as mean±SD, n=3. Absorption percentages were compared to absence of verapamil group. *P□0.05, **P□0.01, ***P□0.001.

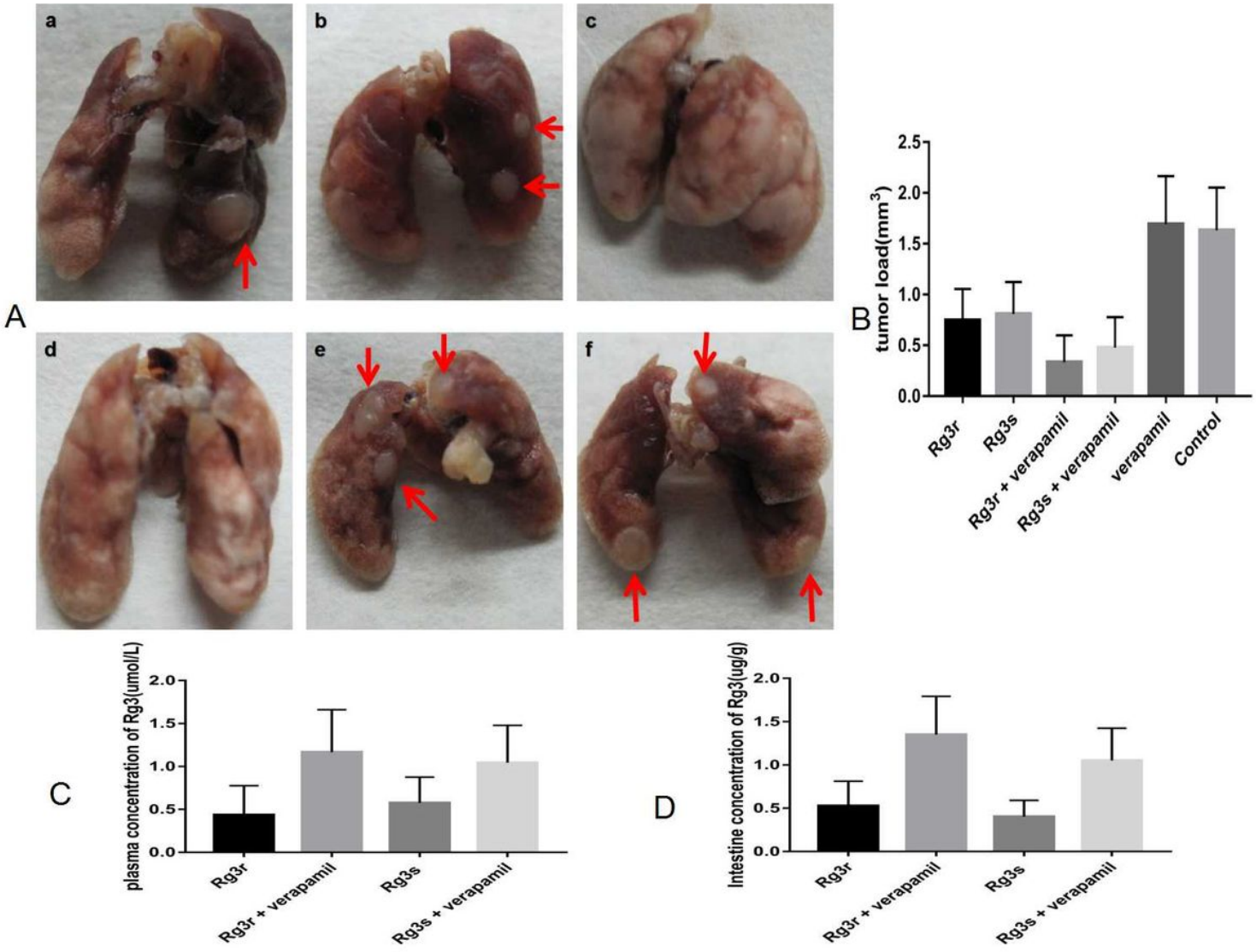

Figure 4

Effects of ginsenoside Rg3 on tumor load, and plasma or intestine concentrations of Rg3 in different groups. (A) Gross lung tumors in A/J mice treated with Rg3 and Rg3 combined with verapamil. Arrows indicate tumors. a: Rg3r group. b: Rg3s group. c: Rg3r combined with verapamil. d: Rg3s combined with verapamil. e: verapamil group. f: Control group. (B) Effects of ginsenoside Rg3 or Rg3 combined with verapamil on tumor load in A/J mice. Error bars represent the mean ± SD of three independent experiments. (C) Plasma concentrations of Rg3r and Rg3s in different groups. Error bars represent the mean ± SD of three independent experiments. (D) Intestine concentrations of Rg3r and Rg3s in different groups. Error bars represent the mean ± SD of three independent experiments.